Metallic Helix Array as a Broadband Wave Plate

Chao Wu, Hongqiang Li,* Xing Yu, Fang Li, and Hong Chen
Key Laboratory of Advanced Micro-structure Materials, MOE, Department of Physics, Tongji University, Shanghai 200092, China

C. T. Chan
Department of Physics, Hong Kong University of Science and Technology, Clear Water Bay, Kowloon, Hong Kong, China
(Received 30 May 2011; published 18 October 2011)

This study demonstrates theoretically and experimentally that a metallic helix array can operate as a highly transparent broadband wave plate in propagation directions perpendicular to the axis of helices. The functionality arises from a special property of the helix array, namely, that two branches of elliptically right-handed and left-handed polarized states are nearly rigidly shifted in frequency and their dispersions are controlled by different mechanisms that can be independently tuned by structural parameters.

DOI: 10.1103/PhysRevLett.107.177401 PACS numbers: 78.67.Pt, 42.25.Ja, 42.70.Qs

Manipulating the polarization of electromagnetic (EM) waves is instrumental in both fundamental optical physics and photonics applications. A wave plate, in the form of a birefringent crystal with specific orientation and thickness, has long been used for the purpose of polarization control. It transforms the polarization of EM waves by the superposition of two linearly polarized states that are orthogonal to each other propagating inside the crystal with different phase velocity [1]. The two orthogonal states can also be, alternatively, left-handed and right-handed elliptically polarized (LEP and REP) eigenstates of uniaxial bianisotropic medium [2]. It is worth noting that such a wave plate with a certain thickness can only operate in a narrow frequency range [1,2] as the difference of phase velocity of two polarized eigenstates is frequency dependent. To build a broadband wave plate with a homogeneous medium, it requires not only that the difference of phase velocity but also the axis ratios of the two polarized states must not change throughout the whole operational band. To the best of our knowledge, no natural or artificial medium exhibits such properties.

Metamaterials have great potential in offering a variety of novel functionalities, such as negative refraction [3], super lens [4,5] invisibility cloak [6,7], and polarization control via chiral route [8–12]. The concept of metamaterial presents a paradigm to create novel EM materials in a form of artificial meta-atom ensemble [13,14]. The crux of the matter relies on how to tailor the EM responses and mutual coupling between the electric field and magnetic field in metamaterial [15]. However, most metamaterials only operate in a narrow frequency range due to local resonance nature. One goal to be achieved is to find metamaterial alternatives for related photonic devices with superior performance much beyond the natural material limits. A helix array, as one classical representative in chiral metamaterials, is also very unique in that the EM properties of such a structure are the collective effect between the local resonance that governs metamaterials and Bragg scattering that governs photonic crystals [16–18].

In this Letter, we show that the helical symmetry of helices provides additional degrees of freedom for tuning the dispersion branches in different handedness, namely, the REP and LEP eigenstates on the transverse plane of metallic helix array are controlled, respectively, by Bragg scattering and the EM coupling derived from the continuous helical symmetry. The ellipticity and difference between wave vectors of the two states can be fixed in a wide frequency range by choosing appropriate geometric parameters, leading to a helix solution for highly transparent broadband wave plate. The proof-of-principle microwave experiments, in good agreement with theoretical calculations, verify the thickness-dependent polarization character of transmitted waves through three helix samples. This is a first realization of a broadband wave plate which utilizes the LEP and REP states of metallic helix array.

Figure 1 presents the schematic configuration of a wave plate made with right-handed (RH) metallic helix array [Fig. 1(a)], a photo of the 7-layered slab sample, the corresponding dispersion diagram $\omega(k_x, k_y = k_z = 0)$ [Fig. 1(b)], and the comparative results by varying critical geometric parameters associated with helical symmetry and Bragg scattering [Figs. 1(c) and 1(d)]. The geometric parameters of the sample shown in Fig. 1(a) are the pitch $p = 4$ mm, the helix radius $a = 3$ mm, the wire diameter $\delta = 0.6$ mm, and the lattice constant $d = 11$ mm. As the helical symmetry requires that a RH helix comes back to itself after being translated by a distance of Δz and being rotated simultaneously by an angle of $2\pi\Delta z/p$ with p being the pitch size, the field components for an RH helix system can be expanded by functions of the form, i.e., the helical Bloch states, as $\psi_n(\rho, \varphi, z) = e^{ik_z z} F_n(\rho) e^{-in\varphi + 2n\pi z/p}$, where k_z is the Bloch wave vector along z axis, and n is the Bloch order associated with angular momentum [18]. Our calculations show that the

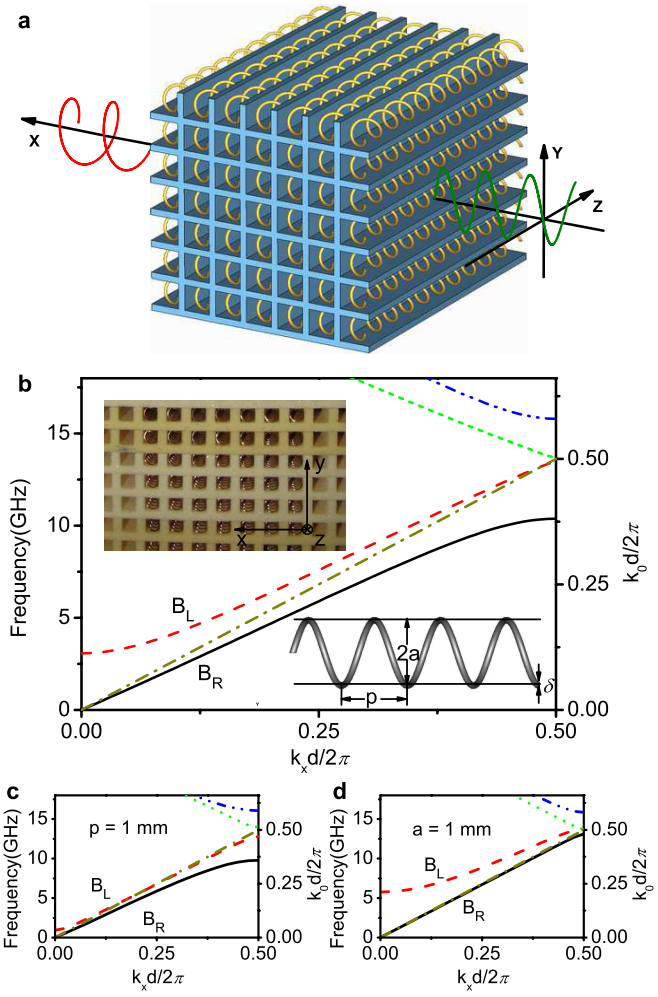

FIG. 1 (color online). A Slab of helices as wave plate for transversely propagating waves. (a) The schematic configuration of transverse propagation through helices, the helices are arranged in a square array; (b) the photo of the 7-layered sample and the corresponding dispersion diagram $\omega(k_x, k_y = k_z = 0)$. The geometric parameters are the pitch $p = 4$ mm, helix radius $a = 3$ mm, wire diameter $\delta = 0.6$ mm, the lattice constant $d = 11$ mm; and the comparative results by (c) varying pitch only to $p = 1$ mm, and (d) varying helix radius only to $a = 1$ mm, all other parameters are fixed to their respective values in Fig. 1(b).

lowest branch B_R [black solid line in Fig. 1(b)] is dictated by the degenerate $\pm$first orders of helical Bloch states with the electric fields along the y direction, while the second lowest branch B_L [red dashed line in Fig. 1(b)] is dictated by the zeroth order of helical Bloch state with the electric fields along the helix axis [18]. Consequently, a B_R/B_L state shall pick up an REP/LEP character with long axis along the y/z direction, as revealed by the polarization analysis of eigenmodes (see Fig. 2). The electric field of two orthogonal elliptical states $|\varphi_{\mathrm{LEP}}\rangle$ and $|\varphi_{\mathrm{REP}}\rangle$ propagating along x axis can be expressed as

$$E_{\mathrm{REP}} = (\alpha u_y + i\beta u_z)e^{i(k_{\mathrm{REP}}x-\omega t)}, \quad (1)$$

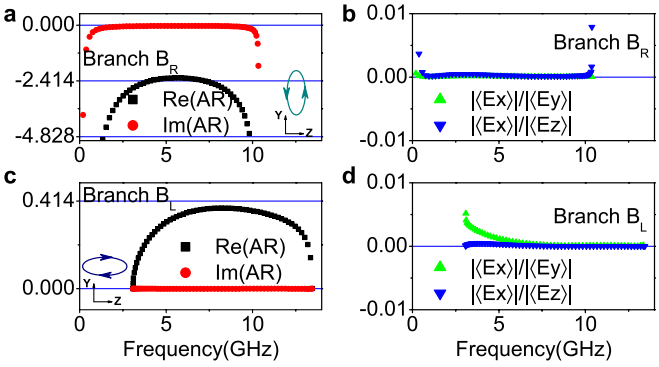

FIG. 2 (color online). Polarization characters of eigenmode. Axial ratio $AR = \langle E_y\rangle/\langle iE_z\rangle$, and longitudinal ratios $|\langle E_x\rangle|/|\langle E_y\rangle|$, $|\langle E_x\rangle|/|\langle E_z\rangle|$ are calculated for (a), (b) B_R, and (c), (d) B_L modes. Black squares for Re(AR), red circles for Im(AR), green up-triangles for $|\langle E_x\rangle|/|\langle E_y\rangle|$, and blue down-triangles for $|\langle E_x\rangle|/|\langle E_z\rangle|$. $\langle\cdots\rangle$ denotes the spatial average in a unit cell.

$$E_{\mathrm{LEP}} = (\beta u_y - i\alpha u_z)e^{i(k_{\mathrm{LEP}}x-\omega t)}, \quad (2)$$

where α and β are two different positive numbers that determine the axis ratio of elliptical states, u_y and u_z denote the unitary vectors along the y and z coordinate axes.

A salient feature of the band structure shown in Fig. 1(b) is that the B_L and B_R branches are essentially linear and parallel to each other in a wide frequency range of 3.9–9.6 GHz. Within this band, two orthogonal eigenstates $|\varphi_{\mathrm{LEP}}\rangle$ and $|\varphi_{\mathrm{REP}}\rangle$ of the B_L and B_R branches pick up the same difference $\Delta k = k_{\mathrm{REP}} - k_{\mathrm{LEP}}$ between their wave vectors. The analysis of equifrequency surfaces (EFS) in Fig. 3 indicates that this property generally holds for all directions in the transverse plane as if the helix array behaves as an isotropic medium for the transversely propagating waves. We also note that, within the same frequency range, the axial ratio of the in-plane field components for the LEP/REP branch [Fig. 1(b)] is roughly fixed as well (see Fig. 2). These properties are adequate for producing a broadband wave plate which surpasses the narrow bandwidth limitation of a birefringent crystal as wave plate.

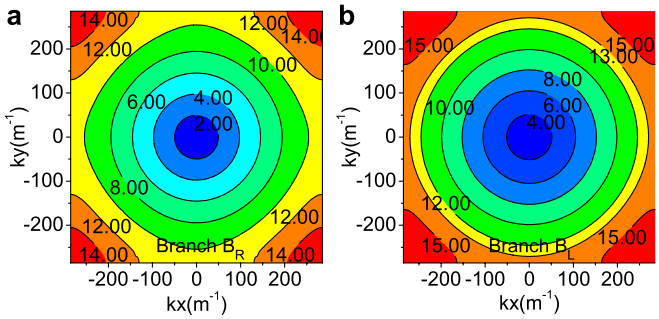

FIG. 3 (color online). Equifrequency surfaces of the BR and BL branches in Fig. 1(b).

It is interesting to note that the dispersions of the B_L and B_R branches can be modulated to be in parallel to each other in a wide frequency range. This is because they are controlled by the EM coupling along the helix (z) axis and the Bragg scattering (in the xy plane), respectively, and the two different mechanisms can be independently modulated by different sets of structural parameters. Such a property is not likely to be found in other systems. We see from Figs. 1(b)–1(d) that the branch B_R, nearly linear at small values of wave vector k_x, opens up a Bragg gap at Brillouin zone (BZ) boundary with the fourth branch (blue dash-dotted line) in the same handedness. On the other hand, the branch B_L has a locally resonant manner with a cutoff frequency at $k_x = 0$, but becomes linear quickly at a finite value of k_x, and meets with the third lowest branch of the same handedness at the BZ boundary without opening a noticeable gap.

Results shown in Fig. 1 for various parameters explicitly demonstrate that the two branches can be tuned independently. The slope of the B_L branch can be larger or smaller than that of the B_R branch, as shown in Figs. 1(c) or 1(d), and they can be made nearly parallel to each other for an appropriate set of geometric parameters like those illustrated in Fig. 1(b). If we only decrease the pitch p, for example, from 4 to 1 mm [see Fig. 1(c)], the cutoff frequency of the B_L branch at $k_x = 0$ falls down to a rather lower frequency as compared to the $p = 4$ mm case [Fig. 1(b)]. We also see that the line shape of B_R branch is almost unchanged as the pitch contributes little to the in-plane Bragg scattering of metallic helix array. On the other hand, if we only decrease the helix radius a, for example, from 3 to 1 mm [Fig. 1(d)], the helix system adopting a smaller size of radius a tends to regress to a two-dimensional array of thin metallic wires. We can see from Fig. 1(d) that the cutoff frequency of the B_L branch goes higher rapidly, while the B_R branch becomes more asymptotic to light line due to weaker Bragg scattering effect as the filling ratio of metallic helices is smaller. In principle, we need only tune the B_L branch by varying the pitch p, or alternatively only tune the B_R branch by varying the helix radius a and holding the ratio of a/p to be fixed, and the ellipticity of eigenstates can also be tailored much in the same way (See Supplemental Material [19] for more details.)

Consider, for example, a linearly polarized plane wave propagating along x direction through the helices with a polarization angle of θ with respect to y axis [see Fig. 1(a)]. The polarization of the outgoing wave [2] can be identified by its axial ratio $ar = E_y/iE_z$ as

$$ar = \frac{(i\alpha/\beta + \tan\theta)e^{-i\Delta k\cdot L} + (i\beta/\alpha - \tan\theta)}{-(i + \beta/\alpha\tan\theta)e^{-i\Delta k\cdot L} + (i - \alpha/\beta\tan\theta)}, \quad (3)$$

where L is the slab thickness. The transmitted waves will be transformed to be right-handed or left-handed circularly polarized (RCP or LCP) at $\theta = 0$ or $\theta = \pi/2$ provided that the axial ratios of REP and LEP eigenstates and the thickness of helix slab satisfy to $\alpha/\beta = \sqrt{2} + 1$ and $\Delta k \cdot L = \pi$, as shown in Fig. 4(a). And the sample shown in the inset of Fig. 1(b), which has 7 periods along x direction, is rightly the realization of such a wave plate with appropriately designated geometric parameters. We would further address that such a helix slab can also rotate linear polarization in a wide frequency range. At the conditions $\Delta k \cdot L = \pi$ and $\theta = \pm\pi/4$, the transmitted wave is still linearly polarized but with rotated polarization direction along $\mp\pi/4$. This property is independent from the axial ratio of elliptical eigenstates as shown in Figs. 4(a) and 4(b). In contrast, a conventional wave plate is incapable of implementing the aforementioned two different kinds of polarization transformation simultaneously. All the predictions in this Letter are made under the assumption of perfect electric conductor for metals which should be a good approximation up to THz frequency and should be qualitatively correct in IR. In the visible regime, the EM fields will penetrate inside the metal, which will abate the chiral effect that is crucial for the broadband utility.

We perform transmission measurements inside an anechoic chamber through a slab of the helix array with the aforementioned geometric parameters [the band structure is shown in Fig. 1(b)]. Helix samples are fabricated by periodically embedding the clockwise metallic helices in a polyurethane foam slab which is nearly lossless with a dielectric constant of $\varepsilon \approx 1.01$. According to the calculated band structure in Fig. 1(b), the thinnest wave plate for linear-to-circular polarization transformation (or vice versa) only requires 7 periods along the x direction. The sample slab contains 7×60 metallic helices (i.e., 7 periods along the x direction and 60 periods along the y direction), each helix has 200 periods along the helix axis. For comparison, finite-difference-in-time-domain algorithm is performed to calculate the transmission spectra. Both the calculations and measurements demonstrate that the transmitted waves are transformed to be RCP or LCP, respectively, under y-polarized or z-polarized incidence as shown with the solid lines and dashed lines in Figs. 5(a) and 5(b).

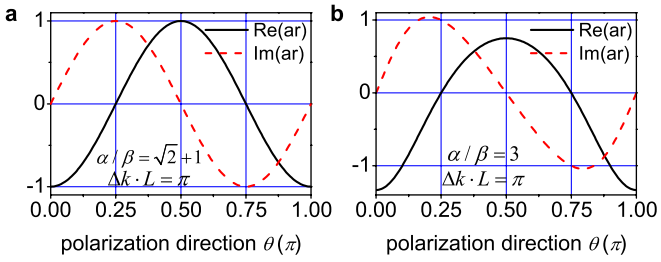

FIG. 4 (color online). Polarization transformation. Axial ratio ar of the transmitted waves as a function of the polarization angle of linearly polarized incidence when the slab thickness satisfies to $\Delta k \cdot L = \pi$ and the ellipticity of the eigenstates is at (a) $\alpha/\beta = \sqrt{2} + 1$ or (b) $\alpha/\beta = 3$. The ratio ar is defined as $ar = E_y/iE_z$, similar to the axial ratio for eigenstates illustrated in Fig. 2.

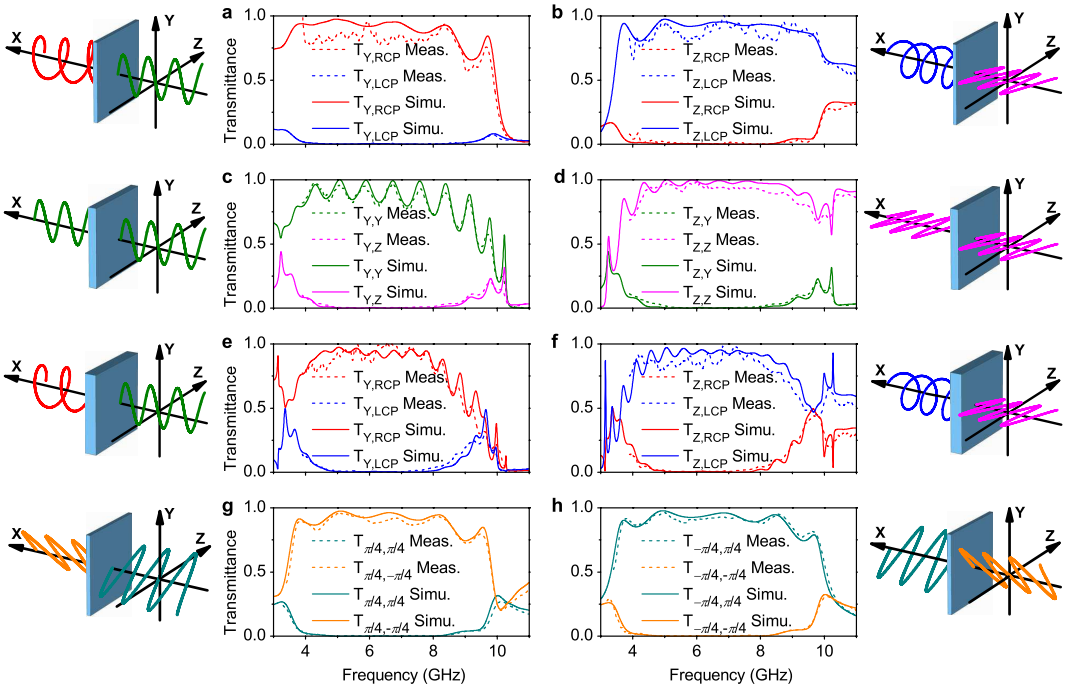

FIG. 5 (color online). Transmission spectra of helix samples as wave plate. Transmission spectra are calculated and measured for three samples with 7, 14, and 21 periods along the propagating direction (x direction). (a) and (b), (g) and (h) for 7-period sample, (c) and (d), (e) and (f) for 14-, 21-period samples, respectively. The first and the second subscripts, i, and j, of the transmission spectra $T_{i,j}$ refer to the polarized state of the incident and the transmitted waves, respectively. The letter Y or Z denotes a linear polarization along y or z direction. The symbol $\pi/4$ or $-\pi/4$ denotes linear polarization with a polarization angle at $\pi/4$ or $-\pi/4$ about y axis. The transmission spectra are normalized to the total power of the incidence.

The calculated or measured transmittance is above 95%/85% at most of the frequencies in the range of 3.9–9.6 GHz. Measured results show that the signal-to-noise ratios ($T_{Y,\mathrm{RCP}}/T_{Y,\mathrm{LCP}}$ or $T_{Z,\mathrm{LCP}}/T_{Z,\mathrm{RCP}}$) are larger than 20 dB in the frequency range of 4.1–8.8 GHz. Note that this entity only relies on intrinsic response of metallic helix array as an artificially made chiral material. And the performance can be much improved by tuning the structural parameters of helix array. As the functionality of a wave plate is thickness dependent, we also fabricated the 14- and 21-period sample slabs with the same geometric parameters in Fig. 1(b). Following the analysis stated above, these two samples shall bring 2π and 3π phase difference between the LEP and REP states, respectively. As such, the sample with 14 periods shall not change the polarization of incident waves, and the functions of the 21-period sample shall be similar to the 7-period one. Calculated and measured transmission spectra shown in Figs. 5(c)–5(f) agree with our predictions very well. The functionality of the 7-layered sample rotating the polarization direction of a linear polarized wave is also illustrated in Figs. 5(g) and 5(h). We can see that the polarization angle of linear polarized wave is perfectly transformed from $\theta = \pm\pi/4$ to $\theta = \mp\pi/4$ as predicted.

Most conventional wave plates, such as those utilizing the birefringence effect of liquid crystals, typically rely on the stacking of different wave plates and system optimizing to extend the operation bandwidth at the cost of transmission attenuation. Here, we provide an entirely new and different strategy for broadband wave plate basing on the unique properties of chiral material. We have shown that, for a metallic helix array, the dispersion branches for opposite handedness can be tuned independently by varying structural parameters. This novel property should be attributed to the additional degrees of freedom associated with continuous helical symmetry of metallic helices, which cannot be found in other systems using natural or other artificial materials. Our findings can be generalized to other frequency regimes such as THz and even the infrared regimes.

This work was supported by NSFC (No. 11174221, No. 10974144, No. 60678046), CNKBRSF (Grant No. 2011CB922001), Hong Kong RGC Grant No. 600209, the National 863 Program of China (No. 2006AA03Z407), NCET (07-0621), STCSM, and SHEDF (No. 06SG24).

*hqlee@tongji.edu.cn

[1] M. Born and E. Wolf, *Principles of Optics: Electromagnetic Theory of Propagation, Interference and Diffraction of Light* (Cambridge University Press, Cambridge, U.K., 1999), 7th ed.

[2] I. V. Lindell *et al.*, *Electromagnetic Waves in Chiral and BI-Isotropic Media* (Artech House, Norwood, MA, 1994).
[3] R. A. Shelby, D. R. Smith, and S. Schultz, Science **292**, 77 (2001).
[4] J. B. Pendry, Phys. Rev. Lett. **85**, 3966 (2000).
[5] D. R. Smith, J. B. Pendry, and M. C. K. Wiltshire, Science **305**, 788 (2004).
[6] J. B. Pendry, D. Schurig, and D. R. Smith, Science **312**, 1780 (2006).
[7] D. Schurig *et al.*, Science **314**, 977 (2006).
[8] A. V. Rogacheva *et al.*, Phys. Rev. Lett. **97**, 177401 (2006).
[9] E. Plum *et al.*, Appl. Phys. Lett. **90**, 223113 (2007).
[10] T. Q. Li *et al.*, Appl. Phys. Lett. **92**, 131111 (2008).
[11] N. Liu *et al.*, Nature Mater. **7**, 31 (2007).
[12] M. G. Silveirinha, IEEE Trans. Antennas Propag. **56**, 390 (2008).
[13] J. Pendry, Nature Mater. **5**, 599 (2006).
[14] N. Liu *et al.*, Nat. Photon. **3**, 157 (2009).
[15] J. B. Pendry, Science **306**, 1353 (2004).
[16] J. K. Gansel *et al.*, Science **325**, 1513 (2009).
[17] J. K. Gansel *et al.*, Opt. Express **18**, 1059 (2010).
[18] C. Wu *et al.*, Phys. Rev. Lett. **105**, 247401 (2010).
[19] See Supplemental Material at http://link.aps.org/supplemental/10.1103/PhysRevLett.107.177401 for theoretical analysis on the characters of B_R and B_L eigenstates, functionality of metallic helix array as a broadband wave plate, and experimental description.